JOURNAL OF GEOPHYSICAL RESEARCH, VOL. 99, NO. D9, PAGES 18,801–18,808, SEPTEMBER 20, 1994

Water activities, densities, and refractive indices of aqueous sulfates and sodium nitrate droplets of atmospheric importance

I. N. Tang and H. R. Munkelwitz

Environmental Chemistry Division, Brookhaven National Laboratory, Upton, New York

Abstract. Water activities, densities, and refractive indices over extended concentration ranges at 25°C are reported for solution droplets containing a single salt of either $(NH_4)_2SO_4$, NH_4HSO_4, $(NH_4)_3H(SO_4)_2$, Na_2SO_4, $NaHSO_4$, or $NaNO_3$, which are common constituents of atmospheric aerosols. The extensive data reported here are obtained from experiments using the single-particle levitation technique recently developed for measuring the thermodynamic and optical properties of microdroplets. These data should find application in mathematical models predicting the dynamic behavior, visibility reduction, and radiative effects of atmospheric sulfate and nitrate aerosols.

Introduction

Inorganic sulfates and nitrates in either pure or mixed forms frequently constitute a major fraction of the ambient aerosol. Both natural and anthropogenic sources contribute to the formation of atmospheric aerosols. It is well known that aerosol plays an important role in many atmospheric processes affecting the local air quality and visibility [*Seinfeld*, 1989; *Sloane and White*, 1986]. Furthermore, *Charlson et al.* [1992] have recently evaluated the source strengths and light-scattering properties of tropospheric aerosols. Their conclusions, as well as other model results [*Charlson et al.*, 1991; *Kiehl and Briegleb*, 1993], all suggest that tropospheric aerosol contributes substantially to radiative forcing and that anthropogenic sulfate aerosol in particular has imposed a major perturbation to this forcing. *Hunter et al.* [1993] subsequently examined patterns of seasonal and latitudinal variations in temperature anomaly trend for evidence of such a perturbation. They found that pronounced minima in the rate of temperature increase during summer months in the northern hemisphere midlatitudes were consistent with both the latitudinal distribution of anthropogenic sulfate and changes in the rate of SO_2 emissions over the industrial era.

Inorganic salt aerosols are mostly hygroscopic by nature and exhibit the property of deliquescence in humid air [*Tang*, 1980]. The phase transformation from a solid particle to a saline droplet usually occurs spontaneously when the relative humidity in the surrounding atmosphere reaches a level, known as the deliquescence humidity, that is specific to the chemical composition of the aerosol particle [*Orr et al.*, 1958; *Tang*, 1976; *Tang and Munkelwitz*, 1993]. Extensive data on water activity and density as a function of solute concentration are required for droplet growth and evaporation computations for aerosols under atmospheric conditions of changing relative humidity. In addition, droplet light-scattering calculations require data on the refractive index as a function of chemical composition [*Tang et al.*, 1981; *Sloane*, 1983; *Larson et al.*, 1988]. Such data are generally available in the literature only for solution concentrations below saturation. Since supersaturated solution droplets are indeed found to be abundant and ubiquitous in the atmosphere [*Rood et al.*, 1989], the need for extending the database beyond saturation concentration is obvious.

In recent years, experimental methods developed for trapping a single micrometer-sized particle in a stable optical or electrical potential well have made it possible to study many physical and chemical properties of aerosol particles. These properties are either unique to small particles or otherwise impossible to measure in bulk samples. A review by *Davis* [1983] has documented the progress up to 1982. Since then, many interesting investigations have appeared in the literature. In particular, the thermodynamic and optical properties of electrolyte solutions at concentrations far beyond saturation that could not have been achieved in the bulk can now be measured with a suspended microdroplet [*Richardson and Spann*, 1984; *Richardson and Kurtz*, 1984; *Tang and Munkelwitz*, 1984, 1991; *Tang et al.*, 1986; *Cohen et al.*, 1987; *Chan et al.*, 1992]. This is accomplished by continuously monitoring the changes in weight and in Mie scattering patterns of a single suspended solution droplet undergoing controlled growth and evaporation, providing extensive data over the entire concentration region. Such data are needed for use as inputs to mathematical models describing the dynamic behavior and radiative effects of atmospheric aerosols [*Hegg et al.*, 1993].

In this paper, water activities, densities, and refractive indices at 25°C are reported for solution droplets containing sulfates or sodium nitrate, $NaNO_3$, which are common constituents of atmospheric aerosol particles. While water activity and density data are presented in the form of polynomials in solute weight percent, the refractive index data are given in the form of partial molal refraction, as was suggested by *Stelson* [1990]. The data formats are chosen so that they can be simply and directly incorporated into modeling computations.

Experimental Procedure

The single-particle levitation technique that was used in this work has been described elsewhere [*Tang et al.*, 1986]. The theory and design of the single-particle levitation cell, also known as electrodynamic balance, have been treated

Paper number 94JD01345.

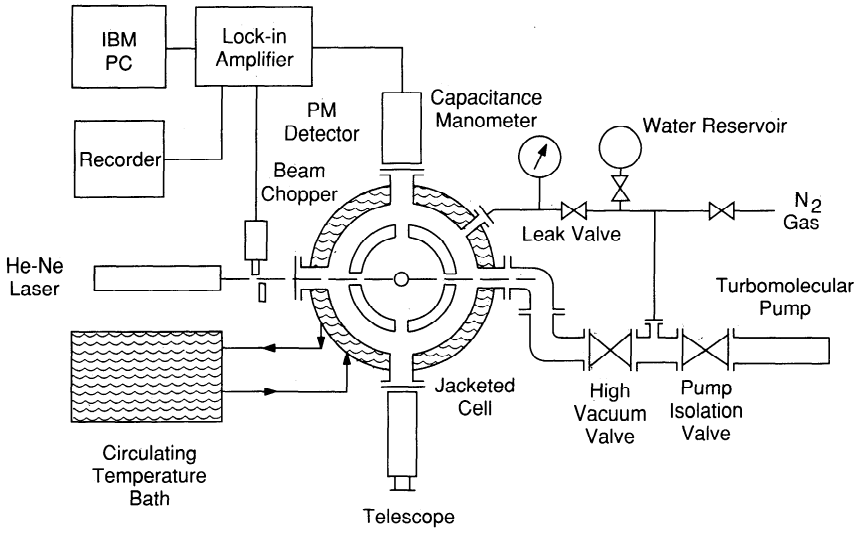

Figure 1. A schematic diagram of the experimental apparatus.

fully by others [*Wueker et al.*, 1959; *Frickel et al.*, 1978; *Davis*, 1983]. A brief description of the apparatus and experimental procedure is presented here.

Apparatus. As is shown in Figure 1, the single-particle levitation cell is placed inside a vacuum chamber equipped with a water jacket that can maintain the cell temperature within ±0.1°C. A linear, vertically polarized He-Ne laser beam enters the cell through a side window and illuminates a charged particle, 6–8 μm in diameter when dry, which is trapped at the null point of the cell by an ac field imposed on a ring electrode surrounding the particle. The particle is balanced against gravity by a dc potential, U, established between two end cap electrodes positioned symmetrically above and below the particle. All electrode surfaces are hyperboloidal in shape and separated by Teflon insulators. When balanced at the null point, the particle mass m is given by

$$m = qU/gz_0 \tag{1}$$

where q is the number of electrostatic charges carried by the particle, g is the gravitational constant, and z_0 is the characteristic dimension of the cell. It follows that the relative mass changes as a result of water vapor condensation or evaporation can be measured as precisely as one can measure the dc voltage changes necessary for restoring the particle to the null point.

In addition to the dc voltage, the laser light intensity scattered from an evaporating droplet is also monitored continuously with a photomultiplier tube that is placed at a 90° angle to the incoming laser, as also shown in Figure 1. The laser beam, which is mechanically chopped at a fixed frequency, is focused on the particle so that a lock-in amplifier can be used to achieve the highest possible sensitivity. Data are routinely taken with an IBM PC.

Procedure. Initially, a charged particle is obtained from a filtered solution of known composition that is loaded in a particle gun, injected into the cell, and captured in dry N_2 at the center of the cell by properly manipulating the ac and dc voltages applied to the electrodes. The system is closed and evacuated to a pressure below 10^{-7} torr. The vacuum is then valved off, and the system is back filled with water vapor to about 5 torr. The dc voltage required to position the particle at the null point is now noted as U_0. A digital voltmeter is used to measure the voltage to within 1 part in 5000. After U_0 has been established, additional water vapor is slowly admitted into the system until the particle deliquesces, as is evidenced by a sudden increase in the dc voltage. As the pressure is further increased, the droplet grows in size by water vapor condensation. The dc voltage U that is required to balance the droplet at the null point at a given time is taken, together with the system water vapor pressure p. Equilibrium is ensured by increasing the system pressure slowly, as discussed elsewhere [*Tang et al.*, 1986]. Thus the ratio U_0/U represents the solute mass fraction, and the ratio p/p^0 represents the corresponding water activity a_w at that point. Here, p^0 is the vapor pressure of water at the system temperature. As the water vapor pressure is gradually reduced by evacuation, droplet evaporation takes place until the humidity becomes low enough and suddenly the droplet crystallizes, expelling all its water content. This is evidenced by an abrupt change in the dc voltage at the end of an experiment. The measurement can be repeated several times with the same particle by simply raising the water vapor pressure again and repeating the cycle. The reproducibility is better than ±2%. Concurrently, the 90° light scattering caused by the suspended particle is recorded continuously during its growth and evaporation.

For a few cases when density and refractive index data were not available in the literature for comparison with the droplet results, separate experiments were carried out to obtain the necessary aqueous solution data. Thus density measurements were made using glass pycnometers whose volumes were calibrated with mercury at specific temperatures. Refractive index measurements were made with a Bausch and Lomb Abbe-3l refractometer equipped with a circulating thermostat.

Results and Discussion

Water activity and aerosol phase transformation. As was mentioned above, atmospheric aerosol particles undergo processes of phase transformation, droplet growth, and

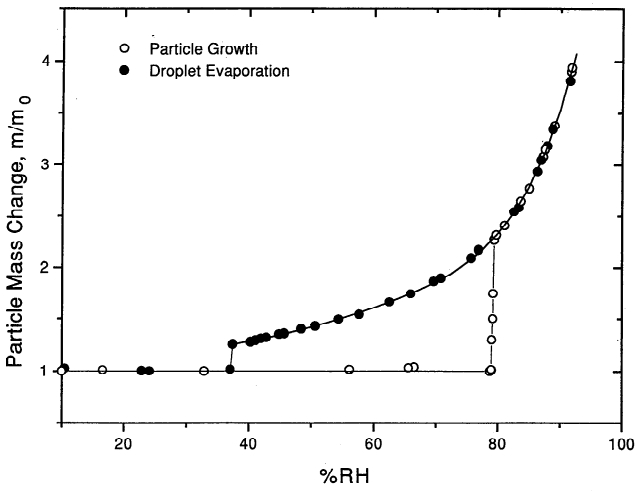

Figure 2. Phase transformation, growth, and evaporation of an $(NH_4)_2SO_4$ particle as a function of relative humidity (RH).

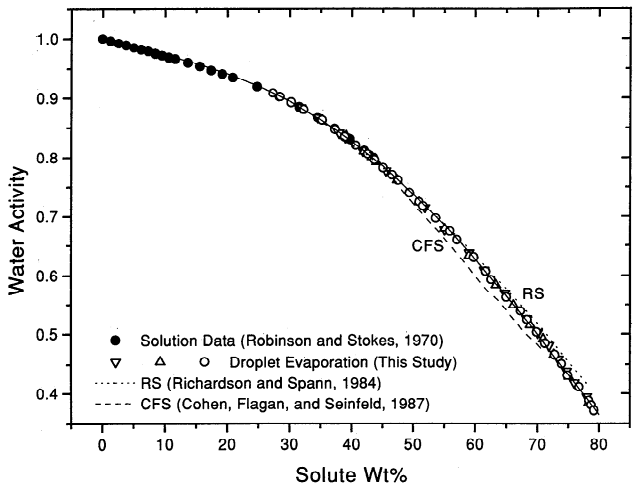

Figure 3. Water activities of aqueous $(NH_4)_2SO_4$ solutions at 25°C.

evaporation when the ambient relative humidity is changing. Figure 2 illustrates how the mass of an ammonium sulfate $[(NH_4)_2SO_4]$ particle changes under the influence of relative humidity. Here the open circles represent measurements when the relative humidity is increasing, whereas the closed circles are points with decreasing relative humidity. It is shown that a solid $(NH_4)_2SO_4$ particle, upon exposure to increasing humidity, will deliquesce to form a solution droplet at the saturation point of 80% relative humidity. Here, percent relative humidity is defined as $100p/p^0$, or $100a_w$. The droplet will continue to grow by water vapor condensation as the relative humidity increases further. When the relative humidity decreases, the droplet will evaporate, pass the saturation point, and continue to evaporate in the supersaturated concentration region. It will suddenly crystallize at about 37% relative humidity. For a droplet whose diameter is greater than 0.1 μm, the Kelvin effect is negligible. Thus the water activities measured in this work with droplets whose diameters typically vary between about 25 and 12 μm during evaporation are solution thermodynamic properties independent of droplet size and not altered by inert gas, if present.

However, the supersaturated solution, as shown here for $(NH_4)_2SO_4$ between 37% and 80% relative humidity, is the metastable state, which exists invariably in aerosol droplets but only to a limited extent in bulk solutions. In order to make droplet growth and evaporation calculations, it is therefore essential to have water activity data for the supersaturated concentration region much beyond the saturation point. Such data were not available until recently, when the single-particle levitation technique was developed.

Richardson and Spann [1984] made water activity measurements at room temperature with $(NH_4)_2SO_4$ solution droplets levitated in a chamber which can be evacuated and back filled with water vapor. On the other hand, *Cohen et al.* [1987] employed an electrodynamic balance placed in a continuously flowing gas stream at ambient pressure and made water activity measurements for a number of electrolytes, including $(NH_4)_2SO_4$. The two sets of data show some discrepancies, which amount to 0.04–0.05 in water activities or 5–6 wt % at high concentration. Because of the atmospheric importance of this system, we decided to repeat the measurement in our apparatus, which is closer in design to that of Richardson and Spann but better thermostatted. Our results, together with those of previous studies, are shown in Figure 3. It appears that although our data seem to agree better with those of Richardson and Spann, the agreement among all the data sets is rather good and acceptable. The discrepancies could be due to experimental uncertainties in balancing the particle at the null point, adverse effects of thermal convection in the cell, and unavoidable humidity and temperature measurement errors as well.

Ammonium bisulfate, NH_4HSO_4, and letovicite, $(NH_4)_3H(SO_4)_2$, are the two other sulfate species commonly found to be present in atmospheric aerosol particles when the acidity of the particles is high. *Tang and Munkelwitz* [1977] and *Tang et al.* [1978] measured the water activities of aqueous solutions of these two electrolytes in the undersaturated concentration region. In this work, the water activity data were extended over the entire concentration range up to the critical supersaturation at which crystallization occurred. Figures 4 and 5 show the droplet evaporation data,

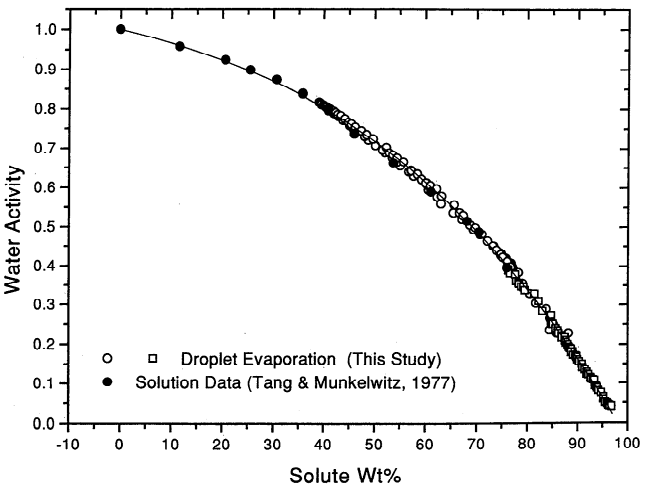

Figure 4. Water activities of aqueous NH_4HSO_4 solutions at 25°C.

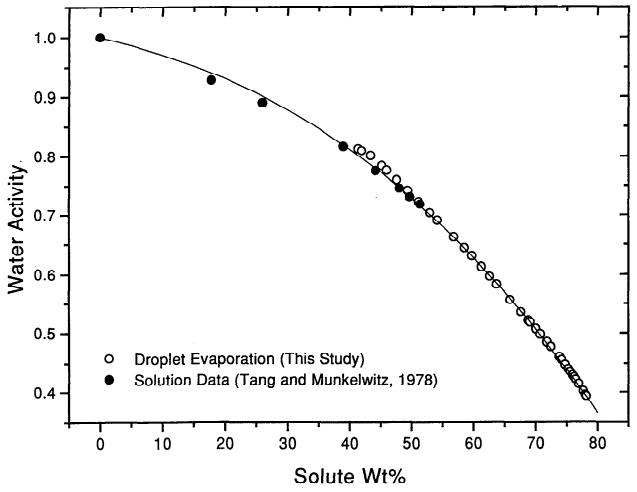

Figure 5. Water activities of aqueous $(NH_4)_3H(SO_4)_2$ solutions at 25°C.

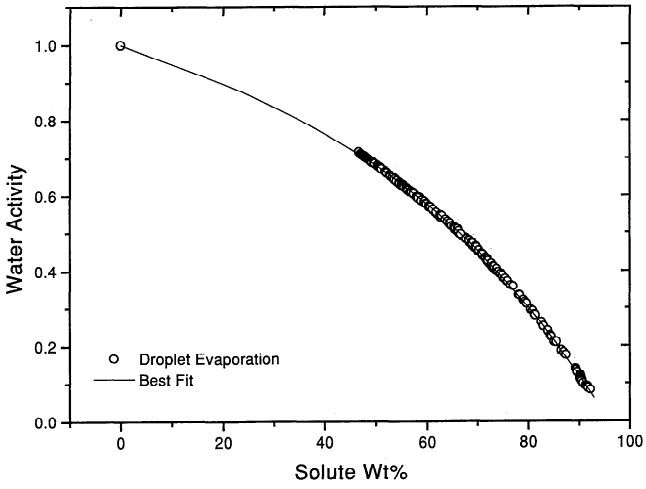

Figure 7. Water activities of aqueous $NaHSO_4$ solutions at 25°C.

together with the previous solution data, for NH_4HSO_4 and $(NH_4)_3H(SO_4)_2$, respectively. It is interesting to observe that, being highly hygroscopic by nature, NH_4HSO_4 solution droplets do not always crystallize readily. Although some solution droplets crystallized at a relative humidity as high as 22%, others were found to remain in the liquid form at 10^{-6} torr for a long time. There are also experimental difficulties in working with these acidic microdroplets. The system must be scrupulously free of ammonia contamination, or the droplet would gain weight by absorbing NH_3 and quickly become $(NH_4)_2SO_4$ or some intermediate species, depending upon the extent of neutralization. *Spann and Richardson* [1985] also reported such experience. Therefore it was our practice to evacuate and bake the system at 75°C overnight before a particle was loaded for measurement. Even so, there was no guarantee that the particle had not absorbed some NH_3, since ammonia is notoriously difficult to remove. The scatter of the data may reflect such an occurrence, but we believe that the data represent the best possible under the present experimental conditions.

Three other electrolytes which are also constituents of atmospheric aerosol particles are included in these studies, namely, sodium sulfate, Na_2SO_4; sodium bisulfate, $NaHSO_4$; and $NaNO_3$. Figures 6–8 present the water activity data for these three salt solutions, respectively. The solution data for each system were taken from the standard reference [*Robinson and Stokes*, 1970], when available. *Cohen et al.* [1987] have reported their droplet evaporation data for Na_2SO_4 and given a polynomial expression derived by combining their measurement with the literature data. Their curve is also shown in Figure 6. It is rather perplexing to observe that, although both data sets show the similar characteristic shape, the difference at high concentration is too large to be within experimental errors. The cause of the discrepancy is not clear. Although the stable form of crystalline sodium sulfate at room temperature is its decahydrate, $Na_2SO_4 \cdot 10H_2O$, the solution droplet under ambient conditions rarely crystallizes to form the hydrate, which should have deliquesced at 93% relative humidity. Instead, it crystallizes into an anhydrous solid particle, which deli-

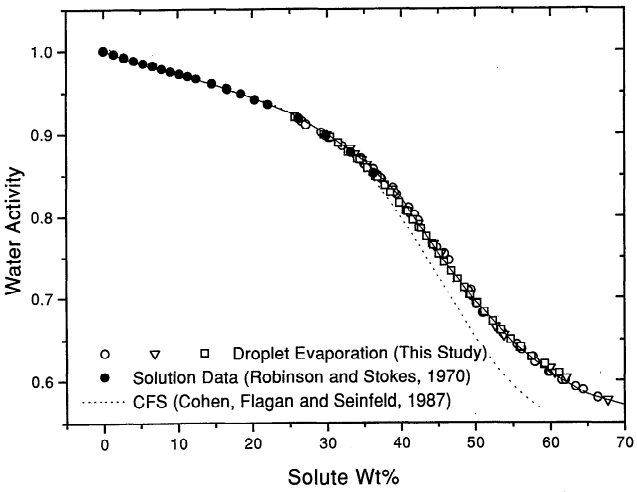

Figure 6. Water activities of aqueous Na_2SO_4 solutions at 25°C.

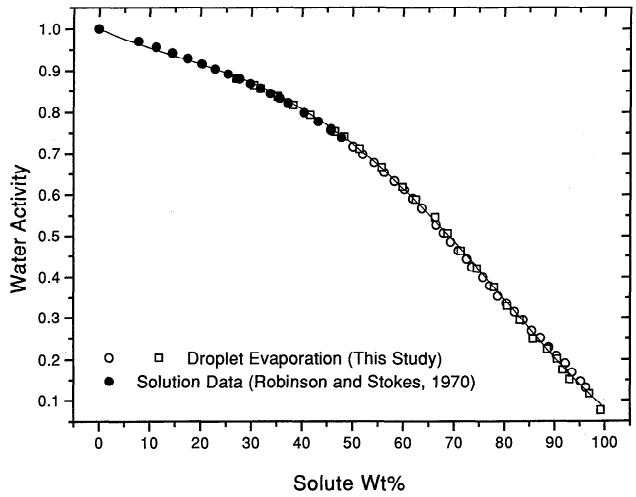

Figure 8. Water activities of aqueous $NaNO_3$ solutions at 25°C.

Table 1. Summary of Polynomial Coefficients for Water Activities and Densities

	$(NH_4)_2SO_4$	NH_4HSO_4	$(NH_4)_3H(SO_4)_2$	Na_2SO_4		$NaHSO_4$	$NaNO_3$
x, %	0–78	0–97	0–78	0–40	40–67*	0–95	0–98
C_1	−2.715 (−3)	−3.05 (−3)	−2.42 (−3)	−3.55 (−3)	−1.99 (−2)	−4.98 (−3)	−5.52 (−3)
C_2	3.113 (−5)	−2.94 (−5)	−4.615 (−5)	9.63 (−5)	−1.92 (−5)	3.77 (−6)	1.286 (−4)
C_3	−2.336 (−6)	−4.43 (−7)	−2.83 (−7)	−2.97 (−6)	1.47 (−6)	−6.32 (−7)	−3.496 (−6)
C_4	1.412 (−8)	...	...	...	...	...	1.843 (−8)
A_1	5.92 (−3)	5.87 (−3)	5.66 (−3)	8.871 (−3)		7.56 (−3)	6.512 (−3)
A_2	−5.036 (−6)	−1.89 (−6)	2.96 (−6)	3.195 (−5)		2.36 (−5)	3.025 (−5)
A_3	1.024 (−8)	1.763 (−7)	6.68 (−8)	2.28 (−7)		2.33 (−7)	1.437 (−7)
$\sigma(a_w)$	2.76 (−3)	7.94 (−3)	5.97 (−3)	3.87 (−3)	3.39 (−3)	3.13 (−3)	6.65 (−3)
$\sigma(d)$	8.98 (−5)	4.03 (−4)	2.13 (−3)	1.71 (−4)		7.55 (−4)	3.83 (−4)

Numbers in parentheses are exponents of base 10 for the coefficients.
*For this concentration range, $a_w = 1.557 + \sum C_i x_i$.

quesces at 84% relative humidity, as observed both in this study and by *Cohen et al.* [1987]. It turns out that the critical supersaturation point at which the droplet crystallizes (at about 58% relative humidity) corresponds to a concentration of about four water molecules per solute, obviously not enough for the formation of decahydrate.

The water activity data shown in Figure 7 for $NaHSO_4$ are those derived from droplet evaporation measurement in this study only. No solution data are known for this electrolyte. $NaHSO_4$ is highly hygroscopic by nature. The solution droplets persisted in vacuum for days without ever crystallizing into a solid particle. In some experiments, a trace amount of a foreign substance such as Na_2SO_4 was added in order to induce nucleation, but to no avail. Therefore its deliquescence and crystallization properties are not known. $NaNO_3$ is also hygroscopic by nature. The solution droplets usually crystallize between 20 and 30% relative humidity. Occasionally, they may persist in the liquid form to a molality as high as 300, at which value one solvent molecule is shared by five or 6 solute molecules!

For each electrolyte solution, a best fit curve, drawn as a solid curve through the data points in Figures 3–8, is represented by the polynomial expression

$$a_w = 1.0 + \sum C_i x^i \tag{2}$$

where x is the solute weight percent and C_i are polynomial coefficients given in Table 1. The numbers in parentheses in Table 1 are exponents of base 10 for the coefficients. Standard deviations, $\sigma(a_w)$, for each polynomial fit are also given in Table 1. For ready reference, some relevant deliquescence and crystallization properties of the systems investigated, except $NaHSO_4$, are summarized in Table 2.

Density and partial molal refraction. In an experiment, the intensity of light scattered from the evaporating droplet is monitored continuously at a 90° angle to the incident laser beam. A typical light-scattering diagram obtained for an aqueous $(NH_4)_2SO_4$ droplet is shown in Figure 9a, revealing minute details of the Mie scattering resonances. As water evaporates from the droplet, the nonvolatile solute becomes increasingly concentrated. As a result, both the density and refractive index of the solution droplet are changing with the droplet concentration. At the end of the experiment, the droplet reaches the critical supersaturation and suddenly transforms into a solid particle. The transition is unmistakably identified not only by a sudden drop in the dc voltage, but also by the noisy light-scattering pattern characteristic of a solid particle.

If the solute concentration in an evaporating droplet is known at any time from the dc measurement, it is possible to deduce the density and refractive index simultaneously from the droplet light-scattering diagram by Mie theory. The computational method has been described elsewhere [*Tang and Munkelwitz*, 1991]. It has also been shown previously in the same reference that the partial molal refraction approach proposed by *Stelson* [1990] for undersaturated electrolyte solutions is equally applicable to supersaturated solutions of $(NH_4)_2SO_4$, Na_2SO_4, and $NaNO_3$, as investigated by the droplet evaporation method. In the present work, the study is extended to cover aqueous solutions of NH_4HSO_4, $(NH_4)_3H(SO_4)_2$, and $NaHSO_4$ over the entire concentration range.

By definition, the molal refraction of either a pure substance or a homogeneous mixture of molal volume V and refractive index n is given by *Moelwyn-Hughes* [1961]:

$$R = V(n^2 - 1)/(n^2 + 2) \tag{3}$$

For a binary solution of solute mole fraction, y, the molal refraction may be expressed as the sum of partial molal refraction of the solvent R_1 and solute R_2 as follows:

$$R = R_1 + (R_2 - R_1)y \tag{4}$$

Table 2. Deliquescence and Crystallization Properties at 25°C

	$(NH_4)_2SO_4$	NH_4HSO_4	$(NH_4)_3H(SO_4)_2$	Na_2SO_4	$NaNO_3$
RHD, %	80	40	69	84	74.5
Solubility, wt%	43.3	76	54	38.5	47.9
RHC, %	40–37	22–0.05	44–35	59–57	30–0.05
Critical supersaturation, wt%	78–80	85–96	75–80	64–69	83–98

Relative humidity at deliquescence and crystallization points is shown as RHD and RHC, respectively.

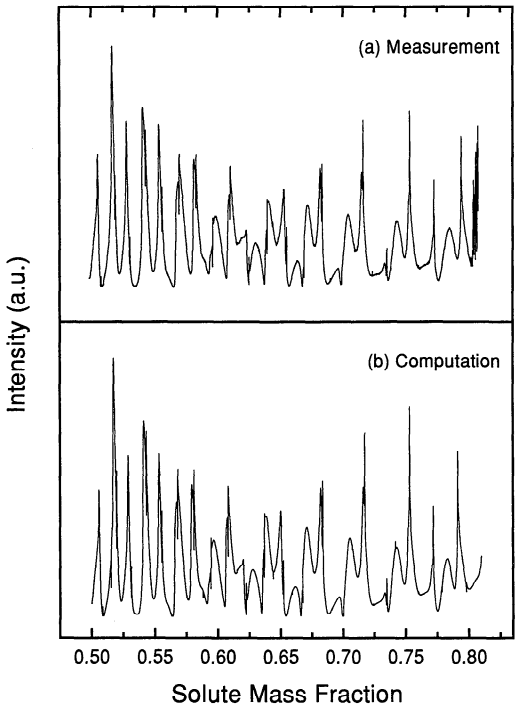

Figure 9. Light-scattering diagram of an evaporating $(NH_4)_2SO_4$ solution droplet (a.u., arbitrary units).

and the molal volume in (3) is given by

$$V = \frac{1}{d}[M_1 + (M_2 - M_1)y] \tag{5}$$

where d is the density of the solution and M_1 and M_2 are the molecular weights of the solvent and solute, respectively. In carrying out Mie computations, the density is expressed by a polynomial:

$$d = 0.9971 + \sum A_i x^i \tag{6}$$

and R_1 is taken as 3.717 for water. By a systematic adjustment of R_2 and the polynomial coefficients A_i, it is possible to arrive at a best fit scattering diagram, as illustrated in Figure 9b for the $(NH_4)_2SO_4$ droplet. It is seen that the computed scattering diagram matches the measured data almost point by point over the entire concentration range. More work is shown in Figure 10, where the measured and computed light-scattering diagrams are compared for an aqueous NH_4HSO_4 droplet evaporating in the high concentration region.

The polynomial coefficients of the densities derived from fitting the light-scattering diagram of an evaporating droplet by Mie theory, together with standard deviations, $\sigma(d)$, are given in Table 1 for aqueous solutions of NH_4HSO_4, $(NH_4)_3H(SO_4)_2$, and $NaHSO_4$, which are the ones investigated in this work. For completeness, data for $(NH_4)_2SO_4$, Na_2SO_4, and $NaNO_3$, taken from *Tang and Munkelwitz* [1991], are also included in Table 1. In separate experiments, some pycnometric and refractometric measurements were made for NH_4HSO_4 and $(NH_4)_3H(SO_4)_2$ solutions at 25°C. The results are given in Table 3. In Figures 11–13, a comparison is shown between the solution data and the droplet evaporation data for the electrolyte solutions of NH_4HSO_4, $(NH_4)_3H(SO_4)_2$, and $NaHSO_4$, respectively. The other three electrolytes have been addressed elsewhere [*Tang and Munkelwitz*, 1991]. In all cases, it is shown that, although the two sets of data are complementary to each other over the entire concentration region, the densities and refractive indices in the supersaturated region may not always be obtained merely by direct extrapolation from the values in the undersaturated region. The droplet evaporation experiments have provided the only high-concentration data.

As was described above, the partial molal refraction of solute can also be derived simultaneously with the density function from the light-scattering diagram of an evaporating droplet. Such data are given in Table 4 for solutions over the entire concentration region. *Stelson* [1990] performed a least squares regression to determine the ionic partial molal refractions from the partial molal refractions of 18 anion-cation combinations of ambient aerosol significance. Again, the density and refractive index data used in the regression are solution data for undersaturated concentrations that are available in the literature. The ionic partial molal refraction is a value assigned to an individual ion so that the partial molal refraction of a neutral electrolyte is the sum of the values of its anions and cations, taking the ionic partial molal refraction to be 0 for the hydrogen ion, H^+. Thus this additivity rule is very useful in determining the molal refraction of an ambient aerosol once the ionic composition is found by chemical analysis. However, according to the definition of molal refraction (equation (3)), the refractive index as a function of composition can only be computed from molal refraction when the droplet density as a function of composition is already known. For systems as complex as

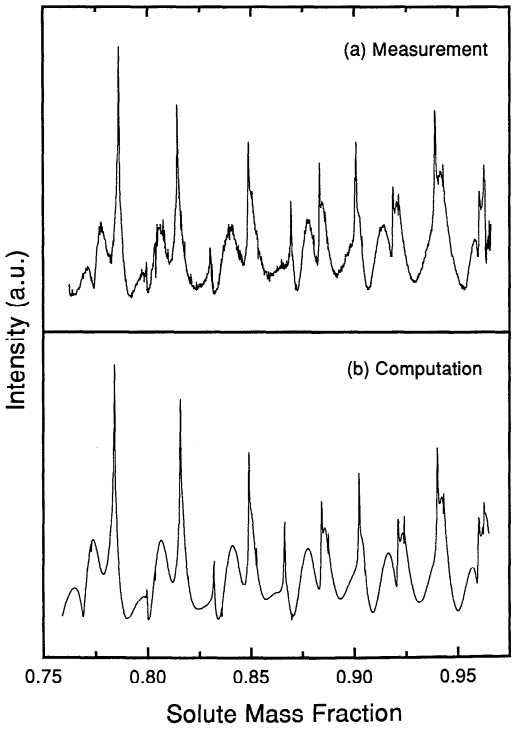

Figure 10. Light-scattering diagram of an evaporating NH_4HSO_4 solution droplet.

Table 3. Densities and Refractive Indices of NH_4HSO_4 and $(NH_4)_3H(SO_4)_2$ Solutions at 25°C

Wt%	Density	Refractive Index
	NH_4HSO_4	
18.09	1.1032	1.3550
18.96	1.1092	1.3560
20.17	...	1.3573
24.63	1.1430	1.3631
34.58	1.2056	...
35.09	1.2085	1.3758
41.99	1.2536	1.3842
49.12	1.3016	1.3927
55.56	1.3470	1.4005
61.86	1.3951	1.4083
	$(NH_4)_3H(SO_4)_2$	
5.89	...	1.3406
6.59	1.0352	...
11.62	1.0638	...
13.48	1.0748	
13.78	...	1.3514
17.96	...	1.3576
18.32	1.1027	...
19.25	1.1077	...
25.90	...	1.3684
28.14	1.1601	...
31.32	...	1.3754
35.21	...	1.3806
35.40	1.2029	...
38.45	...	1.3850
42.83	...	1.3904
46.28	1.2689	1.3949
51.13	1.2989	...

atmospheric aerosols, more work on multicomponent electrolyte solutions is obviously needed.

Nevertheless, the experimental partial molal refraction data obtained in this work can be used to evaluate the ionic partial molal refractions of a few common ions and test the validity of the additivity rule over the extended concentration range. Table 4 summarizes the results of such an evaluation. Also listed in Table 4 are partial molal refractions given by *Stelson* [1990], whenever available. It is seen that

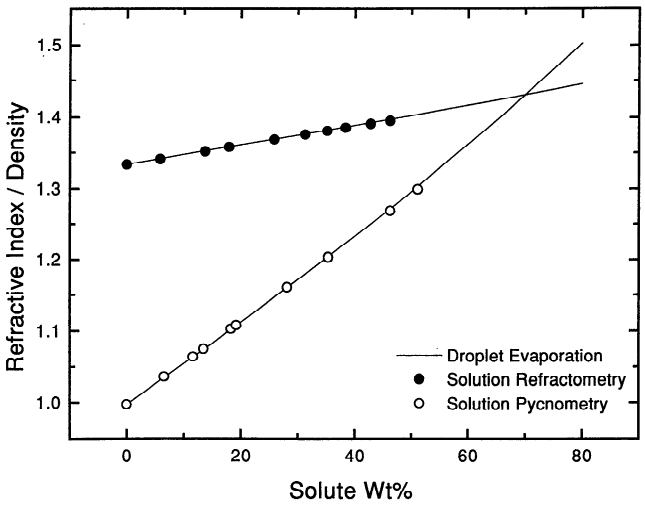

Figure 12. Densities and refractive indices of aqueous $(NH_4)_3H(SO_4)_2$ solutions at 25°C.

molal refractions predicted by the additivity rule from ionic partial molal refractions indeed agree well with measurements over the entire concentration region.

Conclusion

Experimental results are presented for water activities, densities, and partial molal refractions over extended concentration ranges for six sulfate and nitrate species which are major constituents of atmospheric aerosols. The extensive data reported here can only be obtained with the single-particle levitation technique developed recently for measuring the thermodynamic and optical properties of microparticles that are otherwise inaccessible to measurement in bulk samples. Water activity and density data are expressed as polynomials in solute weight percent for the convenience of being readily adopted in modeling computations. Refractive index data are presented as partial molal refractions, a concept that has been validated with electrolyte solution droplets undergoing evaporation over the entire concentra-

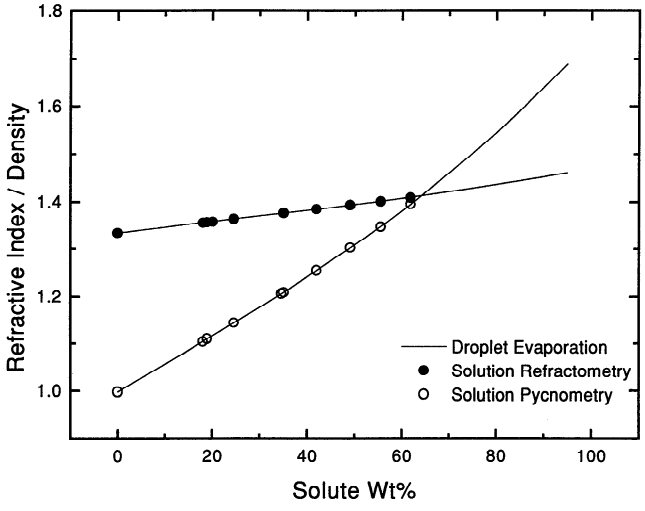

Figure 11. Densities and refractive indices of aqueous NH_4HSO_4 solutions at 25°C.

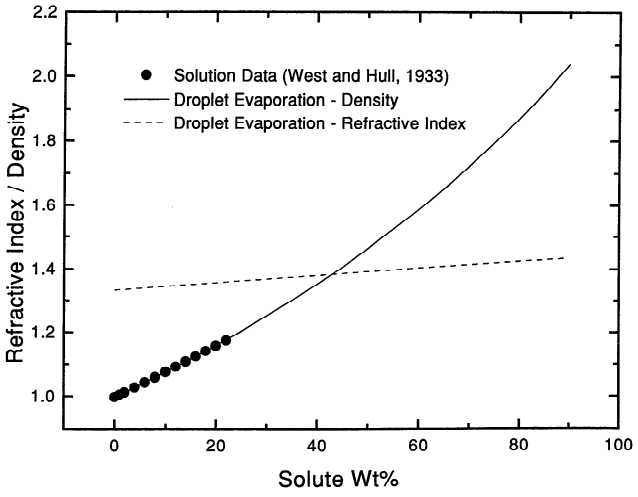

Figure 13. Densities and refractive indices of aqueous $NaHSO_4$ solutions at 25°C.

Table 4. Summary of Partial Molal Refractions of Electrolytes and Ions in Solutions

Electrolyte or Ion	Partial Molal Refraction	
	Literature	This Work
H^+	0	
$SO_4^=$; HSO_4^-	13.45	
NO_3^-	10.19	
NH_4^+	4.89	
Na^+	0.93	
$(NH_4)_2SO_4$	23.27	23.50 ± 0.04
NH_4HSO_4	18.34*	18.38 ± 0.04
$(NH_4)_3H(SO_4)_2$	20.78†	20.95 ± 0.06
$NaNO_3$	11.16	11.22 ± 0.04
Na_2SO_4	15.34	15.13 ± 0.04
$NaHSO_4$	14.38*	14.38 ± 0.06
H_2O	3.712	3.717

Literature values are from *Stelson* [1990] unless indicated otherwise.

*Estimated by using additivity rule.

†Both molecular weight and molal refraction are calculated from $[NH_4HSO_4 + (NH_4)_2SO_4]/2$.

tion region. The data reported here should find application in mathematical models predicting the dynamic behavior, visibility reduction, and radiative effects of atmospheric sulfate and nitrate aerosols.

Acknowledgment. This research was performed under the auspices of the U.S. Department of Energy under contract DE-AC02-76CH00016.

References

Chan, C. K., R. C. Flagan, and J. H. Seinfeld, Water activities of $NH_4NO_3/(NH_4)_2SO_4$ solutions, *Atmos. Environ., Part A, 26*, 1661–1673, 1992.

Charlson, R. J., J. Langner, H. Rodhe, C. B. Leovy, and S. G. Warren, Perturbation of northern hemisphere radiative balance by backscattering from anthropogenic sulfate aerosols, *Tellus, Ser. B, 43*, 152–163, 1991.

Charlson, R. J., S. E. Schwartz, J. M. Hales, R. D. Cess, J. A. Coakley Jr., J. E. Hansen, and D. J. Hofmann, Climate forcing by anthropogenic aerosols, *Science, 255*, 423–430, 1992.

Cohen, M. D., R. C. Flagan, and J. H. Seinfeld, Studies of concentrated electrolyte solutions using the electrodynamic balance, 1, Water activities for single-electrolyte solutions, *J. Phys. Chem., 91*, 4563–4574, 1987.

Davis, E. J., Transport phenomena with single particles, *Aerosol Sci. Technol., 2*, 121–144, 1983.

Frickel, R. H., R. E. Schaffer, and J. B. Stamatoff, Chambers or the electrodynamic containment of charged aerosol particles, *Tech. Rep. ARCSL-TR-77041*, Chem. Syst. Lab., Aberdeen Proving Ground, Md., 1978.

Hegg, D., T. Larson, and P. F. Yuen, A theoretical study of the effect of relative humidity on light scattering by tropospheric aerosols, *J. Geophys. Res., 98*, 18435–18439, 1993.

Hunter, D. E., S. E. Schwartz, R. Wagner, and C. M. Benkovitz, Seasonal, latitudinal, and secular variations in the temperature trend: Evidence for influence of anthropogenic sulfate, *Geophys. Res. Lett., 20*, 2455–2458, 1993.

Kiehl, J. T., and B. P. Briegleb, The relative roles of sulfate aerosols and greenhouse gases in climate forcing, *Science, 260*, 311–314, 1993.

Larson, S. M., G. R. Cass, K. J. Hussey, and F. Luce, Verification of image processing based visibility models, *Environ. Sci. Technol., 22*, 629–637, 1988.

Moelwyn-Hughes, E. A., *Physical Chemistry*, 2nd rev. ed., p. 397, Pergamon, New York, 1961.

Orr, Jr., C., F. K. Hurd, and W. J. Corbett, Aerosol size and relative humidity, *J. Colloid Sci., 13*, 472–482, 1958.

Richardson, C. B., and C. A. Kurtz, A novel isopiestic measurement of water activity in concentrated and supersaturated lithium halide solutions, *J. Am. Chem. Soc., 106*, 6615–6618, 1984.

Richardson, C. B., and J. F. Spann, Measurement of the water cycle in a levitated ammonium sulfate particle, *J. Aerosol Sci., 15*, 563–571, 1984.

Robinson, R. A., and R. H. Stokes, *Electrolyte Solutions*, Butterworth, London, 1970.

Rood, M. J., M. A. Shaw, T. V. Larson, and D. S. Covert, Ubiquitous nature of ambient metastable aerosol, *Nature, 337*, 537–539, 1989.

Seinfeld, J. H., Urban air pollution: State of science, *Science, 243*, 745–752, 1989.

Sloane, C. S., Optical properties of aerosols: Comparison of measurements with model calculations, *Atmos. Environ., 17*, 409–419, 1983.

Sloane, C. S., and W. H. White, Visibility: An evolving issue, *Environ. Sci. Technol., 20*, 760–766, 1986.

Spann, J. F., and C. B. Richardson, Measurement of the water cycle in mixed ammonium acid sulfate particles, *Atmos. Environ., 19*, 819–825, 1985.

Stelson, A. W., Urban aerosol refractive index prediction by molar refraction approach, *Environ. Sci. Technol., 24*, 1676–1679, 1990.

Tang, I. N., Phase transformation and growth of aerosol particles composed of mixed salts, *J. Aerosol Sci., 7*, 361–371, 1976.

Tang, I. N., Deliquescence properties and particle size change of hygroscopic aerosols, in *Generation of Aerosols*, edited by K. Willeke, chap. 7, pp. 153–167, Butterworth, Stoneham, Mass., 1980.

Tang, I. N., and H. R. Munkelwitz, Aerosol growth studies, III, Ammonium bisulfate aerosols in a moist atmosphere, *J. Aerosol Sci., 8*, 321–330, 1977.

Tang, I. N., and H. R. Munkelwitz, An investigation of solute nucleation in levitated solution droplets, *J. Colloid Interface Sci., 98*, 430–438, 1984.

Tang, I. N., and H. R. Munkelwitz, Simultaneous determination of refractive index and density of an evaporating aqueous solution droplet, *Aerosol Sci. Technol., 15*, 201–207, 1991.

Tang, I. N., and H. R. Munkelwitz, Composition and temperature dependence of the deliquescence properties of hygroscopic aerosols, *Atmos. Environ., Part A, 27*, 467–473, 1993.

Tang, I. N., H. R. Munkelwitz, and J. G. Davis, Aerosol growth studies, VI, Phase transformation of mixed salt aerosols in a moist atmosphere, *J. Aerosol Sci., 9*, 505–511, 1978.

Tang, I. N., W. T. Wong, and H. R. Munkelwitz, The relative importance of atmospheric sulfates and nitrates in visibility reduction, *Atmos. Environ., 15*, 2463–2471, 1981.

Tang, I. N., H. R. Munkelwitz, and N. Wang, Water activity measurements with single suspended droplets: The NaCl-H_2O and KCl-H_2O systems, *J. Colloid Interface Sci., 14*, 409–415, 1986.

West, C. J., and C. Hull, *International Critical Tables*, McGraw-Hill, New York, 1933.

Wueker, R. F., H. Shelton, and R. V. Langmuir, Electrodynamic containment of charged particles, *J. Appl. Phys., 30*, 342–349, 1959.

H. R. Munkelwitz and I. N. Tang, Environmental Chemistry Division, Brookhaven National Laboratory, Upton, NY 11973.

(Received January 31, 1994; revised May 3, 1994; accepted May 17, 1994.)